Available online at www.sciencedirect.com
ScienceDirect
Powder Technology 172 (2007) 89–98
POWDER TECHNOLOGY
www.elsevier.com/locate/powtec

Fine particle capture in biomass boilers with recirculating gas cyclones: Theory and practice

R.L.R. Salcedo [a,*], V.G. Chibante [a], A.M. Fonseca [b], G. Cândido [c]

[a] DEQ, Faculdade de Engenharia da Universidade do Porto, R. Dr. Roberto Frias, 4200-465 Porto, Portugal
[b] CEMAS, Universidade Fernando Pessoa, Porto, Portugal
[c] Phillips Portuguesa S.A., Linda-a-Velha, Portugal

Received 25 January 2006; received in revised form 27 June 2006; accepted 17 October 2006
Available online 28 October 2006

Abstract

This paper addresses the theoretical development and experimental validation of optimized recirculating reverse-flow gas cyclones. The simulation of these systems is based on the predictive properties of a finite diffusivity model, modified to include partial recirculation of the cyclones' emissions.

Experimental validation was obtained at laboratory and pilot scales at low temperatures (up to 350 K) and for cork waste biomass boilers at higher temperatures (up to 600 K). Under certain circumstances, with recirculation, the proposed system showed a better performance than an online pulse jet bag filter, and substantially better than with multicyclone systems. The generally observed unexpected high collection of submicron particles, which occurs with inlet concentrations as low as 100 μg/m^3, is attributed to turbulent dispersion, either by promoting fine particle capture by larger ones, much like what occurs in recirculating fluidized beds, or by bringing fine particles near the cyclone wall.

The extremely fine particle size distributions exiting from the recirculation system, as measured off-line at laboratory, pilot and industrial scales, were confirmed at pilot scale using online measurements through a laser monitor.

Keywords: Optimized cyclones; Recirculation; Turbulent dispersion; Fine particles

1. Introduction

Cyclones are gas–solid separation devices used in a wide variety of industries, mainly for the recovery of raw or process materials, as collectors for compliance with particulate emission limits, and as primary collectors for reducing the burden on more expensive secondary collectors. Cyclones are especially attractive for operation at high temperature and/or pressure, where the development of highly efficient devices, especially for fine particles below 2–3 μm in diameter, could have a significant impact in the chemical processing industries [1].

Obtaining high efficiency (HE) cyclones has been essentially an empirical task. However, due to the large dimension of the problem (an 8-degree of freedom problem for optimizing a single reverse-flow cyclone), cyclone improvement through empirical design has been at best moderately successful [4].

The present work deals with the performance evaluation of numerically optimized reverse-flow gas cyclones (RS_VHE geometry, VHE standing for Very High Efficiency), which were designed by solving a numerical optimization problem [2–6]. At the same time, a recirculation system within a collector-first approach, viz. with the reverse-flow cyclone (collector) placed upstream of the straight-through cyclone (concentrator), has also been implemented [6–8]. These systems have been studied at laboratory (≈1 m^3/h), pilot (≈10^3 m^3/h) and industrial (≈ up to 5×10^4 m^3/h) scales.

Previous work [8] shows that cut-points, i.e. particle size captured with 50% efficiency, of 0.3–0.4 μm can be achieved with recirculation systems at laboratory scale with very fine inlet distributions even at very small concentrations (<100 mg/m^3). This paper shows results obtained on the capture of fine lime at laboratory scale, and on three full-scale facilities replacing both multicyclone banks and an online pulse jet bag filter.

For typical emissions from cork and wood waste boilers (median volume diameter ≈8–12 μm), the results obtained

* Corresponding author. Tel.: +351 225081644; fax: +351 225081632.
E-mail address: rsalcedo@fe.up.pt (R.L.R. Salcedo).

0032-5910/$ - see front matter © 2006 Elsevier B.V. All rights reserved.
doi:10.1016/j.powtec.2006.10.027

show that these systems produce, even at industrial scale, extremely fine particle size distribution emissions to the stack (median volume diameter ≈1.5 μm). These fine distributions were confirmed by measurements conducted online at a pilot scale recirculation facility.

2. Optimized reverse-flow gas cyclone and recirculation system

With the purpose of designing a VHE cyclone, a numerical problem was set-up whereby collection efficiency should be maximized subject to several geometric and operating constraints. Previous work [4,9,10] showed that the finite diffusivity simulation model for particle capture under cyclone flow due to Mothes and Löffler [11] gives fair agreement with a large range of experimental grade efficiencies obtained by different authors. Thus, this model was retained as an adequate simulator for cyclone performance, within the framework of performing the numerical optimization of its geometry [4]. The particles' turbulent dispersion coefficient, which is a parameter in the Mothes and Löffler model [11], was predicted for new and unforeseen geometries (which are generated by the numerical optimization code) through an empirical relation between the radial Peclet and Reynolds numbers [3]:

$$Pe_p = 0.0342\ Re_p^{1.263} \tag{1}$$

where $Pe_p = wd_p/\mathcal{D}_r$ is the radial particle Peclet number, $\mathcal{D}_r$ is the radial dispersion coefficient and $Re_p = \rho d_p w/\mu$ is the radial particle Reynolds number. Details of the optimization problem, of the numerical procedure and the resulting cyclone geometry can be found elsewhere [2,4,5].

One way to increase cyclone collection efficiency beyond improving its design is to promote partial recirculation with a straight-through cyclone concentrator. The straight-through cyclone has a tangential inlet for promoting swirl, and both a tangential and axial exits. The tangential exit redirects some particles that escape the reverse-flow cyclone back to it, while the remainder escapes to the atmosphere through the axial exit. A strong swirl is induced in the recirculator as observed by the need to place a vortex breaker downstream of the recirculator, if for example one wishes to measure velocity profiles at that location.

The proposed recirculation system ([6–8], see Fig. 1) differs from those available before [12], since it locates the collector (reverse-flow cyclone) upstream from the concentrator (straight-through cyclone). Recirculation is promoted by some means, such as by a venturi for laboratory scale or by a blower or ejector for industrial scale and high temperature applications. The proposed collector–concentrator sequencing has a global efficiency (η), which depends on the collector and concentrator efficiencies, respectively η_c and η_s, given by:

$$\eta = \frac{\eta_c}{1-\eta_s + \eta_c\eta_s} \tag{2}$$

The system efficiency (η) will be larger than that of the reverse-flow cyclone (η_c), since it is only required that

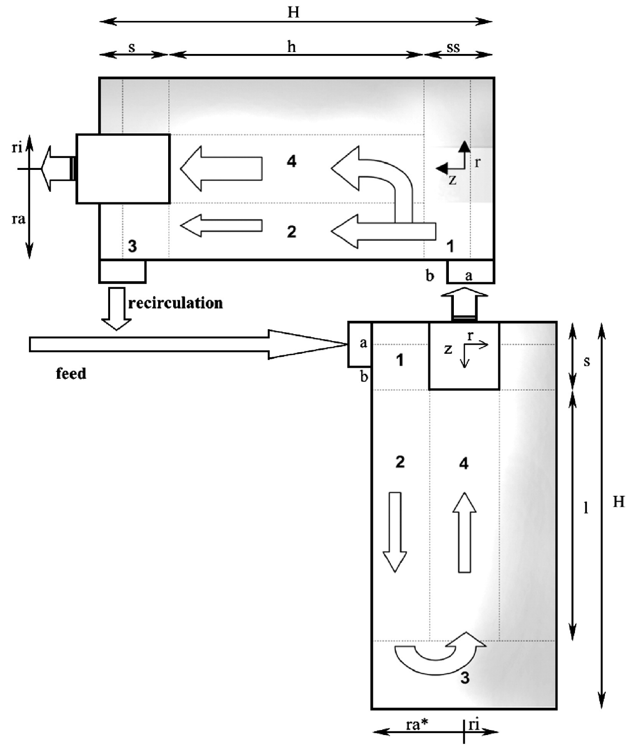

Fig. 1. Geometric model for proposed recirculation system.

$\eta_s(\eta_c - 1) < 0$, which is always verified. It can also be shown [6,7] that the proposed system is always more efficient than the concentrator-first arrangement [12], as long as the individual in-loop efficiencies (collector and concentrator) are the same in both systems.

To model the recirculation system, the reverse-flow cyclone (collector) was approached as a cylinder with the same internal volume as the actual cylinder-on-cone cyclone, such as proposed by Mothes and Löffler. Details are here omitted and can be seen on the original work of these authors [11]. To model the straight-through cyclone (concentrator), the flow is divided in a tangential flow returning to the collector and in an axial flow escaping to the atmosphere (i.e., stack). The overall proposed geometric model is seen in Fig. 1, where the original nomenclature as used by Mothes and Löffler [11] has been retained for an easier understanding. Due to conciseness, only the differing aspects between modeling the concentrator *vs.* the collector will be given here.

Let the entry volumetric flow rate at the concentrator be $\dot{V}_0$ with an inlet particle concentration C_0. The tangential velocity distribution follows a similar radial dependence as for the reverse-flow collector. However, since the cone section does not exist anymore, the parameter K that accounts for the exchange of angular momentum between the wall and the gas is given by:

$$K = \frac{v_{\varphi a}}{v_d}\xi \tag{3}$$

where ξ is an apparent friction coefficient (≈0.007 for smooth-walled cyclones), $v_{\varphi a}$ is the tangential velocity near the wall owing to the *vena contracta* in the entry region, and v_d is the mean barrel velocity $\left(\frac{\dot{V}_0}{\pi r_a^2}\right)$. *Vena contracta* is introduced in the concentrator much like in a tangential inlet reverse-flow cyclone. This work neglects frictional drag on the gas due to the presence of solids, both suspended and collected on the wall.

Fig. 1 shows the concentrator divided into 4 distinct regions. Contrary to what happens in the reverse-flow cyclone model, the entry flow divides and now takes two paths: the exiting axial central flow, and the recirculating peripheral flow, that exits tangentially. The total flow entering the concentrator, V_0, is thus given by $\dot{V}_0=\dot{V}_2+\dot{V}_4$, where $\dot{V}_2=\mathrm{rr}\dot{V}_0$ and $\dot{V}_4=(1-\mathrm{rr})\dot{V}_0$, with rr the ratio of the recirculating flow over the total flow entering the concentrator.

2.1. Entry region — 1

In the entry region, particles move downwards with the gas, and approach the wall at their terminal velocity. The pertinent equations are exactly those of the reverse-flow cyclone, except for $\boldsymbol{r}_a^*$ (cylindrically equivalent cyclone radius) being substituted by $\boldsymbol{r}_a$.

2.2. Region of axial peripheral flow — 2

Here, particle concentration is determined by wall deposition and also by convective and diffusive exchanges with region 4. The net direction for convective particle flow depends on both the particle terminal velocity $\omega(r_i)=\frac{\rho d_p^2 v_\varphi^2(r_i)}{18\mu r_i}$ and gas radial velocity $v_r(r_i)=\frac{\dot{V}_4}{2\pi r_i h}$. The diffusive flow is determined by the particles' concentration gradient between both regions and by the particles' dispersion coefficient. Thus

$$\dot{V}_0\frac{\mathrm{d}C_2}{\mathrm{d}z}=-2\pi r_a\omega(r_a)C_2(z)+2\pi r_i\left[-\mathcal{D}_r\frac{C_2(z)-C_4(z)}{r_a-r_i}\right]+2\pi r_i[\omega(r_i)-v_r(r_i)]C_4(z) \quad (4)$$

where $\mathcal{D}_r$ is the particle turbulent dispersion coefficient. This equation can be simplified by writing:

$$A'=\frac{2\pi r_a\omega(r_a)}{\dot{V}_0};\ B'=\frac{2\pi r\mathcal{D}_r}{(r_a-r_i)\dot{V}_2};\quad C'=\frac{2\pi r_i[\omega(r_i)-v_r(r_i)]_i}{\dot{V}_2} \quad (5)$$

giving:

$$\frac{\mathrm{d}C_2}{\mathrm{d}z}+AC_2(z)-BC_4(z)=0 \quad (6)$$

If $\omega(r_i)\geq v_r\ (r_i)$ then $A=A'+B'$ and $B=C'+B'$, otherwise $A=A'+B'-C'$ and $B=B'$.

2.3. Region of particle capture — 3

Particle capture for the concentrator means particles that are returned to the cyclone with the tangentially recirculated gas flow, and that do not escape with the axial flow. Thus for the concentrator there is truly no region of particle capture, i.e., physical separation from the gas, and this simply means the returning flow from region 2.

2.4. Region of axial central flow (discharge to stack) — 4

In this region,

$$\frac{\mathrm{d}C_4}{\mathrm{d}z}+DC_4(z)-EC_2(z)=0 \quad (7)$$

If $\omega(r_i)\geq v_r(r_i)$ then $D=D'+E'$ and $E=D'$, otherwise $D=D'$ and $E=D'-E'$. The constants D' and E' are obtained by:

$$D'=\frac{2\pi r_i\mathcal{D}_r}{(r_a-r_i)\dot{V}_4};\ E'=\frac{2\pi r_i}{\dot{V}_4}[\omega(r_i)-v_r(r_i)] \quad (8)$$

Eq. (7) may be rewritten as:

$$C_2(z)=\frac{\frac{\mathrm{d}C_4}{\mathrm{d}z}+DC_4(z)}{E} \quad (9)$$

Differentiating once and substituting $C_2(z)$ and $\mathrm{d}C_2/\mathrm{d}z$ in Eq. (7):

$$\frac{\mathrm{d}^2C_4}{\mathrm{d}z^2}+(D+A)\frac{\mathrm{d}C_4}{\mathrm{d}z}+(AD-BE)C_4(z)=0 \quad (10)$$

This is a second-order linear equation whose characteristic equation has roots:

$$\lambda_{1,2}=-\left(\frac{D+A}{2}\right)\pm\sqrt{\left(\frac{D+A}{2}\right)^2-(AD-BE)} \quad (11)$$

Particle concentration in regions 2 and 4 are defined by the general forms:

$$C_4(z)=R_1\exp[\lambda_1(z-ss)]+R_2\exp[\lambda_2(z-ss)] \quad (12)$$

$$C_2(z)=\frac{1}{E}\left\{\begin{array}{l}R_1\lambda_1\exp[\lambda_1(z-\mathrm{ss})]+R_2\lambda_2\exp[\lambda_2(z-\mathrm{ss})]+\\ D\{R_1\exp[\lambda_1(z-\mathrm{ss})]+R_2\exp[\lambda_2(z-\mathrm{ss})]\}\end{array}\right\} \quad (13)$$

With the boundary conditions:

$$C_4(\mathrm{ss})=C_1(\mathrm{ss})\text{ and }C_2(\mathrm{ss})=C_1(\mathrm{ss}) \quad (14)$$

one obtains:

$$R_1=C_1(\mathrm{ss})-R_2\text{ and }R_2=C_1(\mathrm{ss})\frac{E-D-\lambda_1}{\lambda_2-\lambda_1}. \quad (15)$$

2.5. Collection efficiency of the cyclone concentrator

The removal (concentration) efficiency is simply given by:

$$\eta_s=1-\frac{C_4(z=H-s)\dot{V}_4}{C_0\dot{V}_0} \quad (16)$$

Despite the obvious similarities between the model described above for the concentrator and the model of Mothes and Löffler

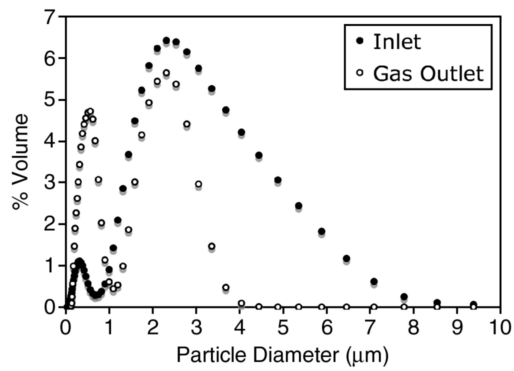

Fig. 2. Average inlet and outlet $Ca(OH)_2$ distributions at recirculation system.

for a reverse-flow cyclone [11], both providing analytical solutions, the model for the entire system is coupled through a varying particle size distribution at the reverse-flow cyclone (collector) inlet, thus requiring some sort of numerical approach. The adopted solution is a direct iterative procedure, whereby the particle size distribution is changed in each pass through the collector and concentrator. Convergence is assumed if the change in mass at the outlet distribution becomes lower than a pre-specified low value, viz. 0.01%, and typically only a few iterations (≈10) are needed. We examine below the behavior of the proposed recirculation system at both laboratory and full scales, and compare it with predictions from the above model.

3. Laboratory scale experiments

The laboratory scale experiments were performed at ambient temperature on a variety of fine dusts using a 0.02 m diameter RS_VHE design. Due to the very small flows involved (≈1 m^3/h), recirculation was achieved by a small ASME venturi (0.002 m throat diameter).

The hydrated lime test dust (Riedel-de-Haën, lot 31219, minimum $Ca(OH)_2$ of 96% and maximum CaCO of 3%) has a median volume diameter of 2.3 μm, specific gravity 2350 kg/m^3, and was injected from a Wright dust feeder [13] at flow rates varying from 2.28 to 4.80×10^{-4} m^3/s, and inlet concentrations of 0.5 to 1.0 g/m^3. These correspond to cyclone mean inlet velocities between 7 and 15 m/s. To avoid the presence of large agglomerates at the test cyclone inlet, a 0.07 m diameter Stairmand HE de-agglomerating cyclone was placed upstream of the test cyclone.

Fig. 2 shows that all particles fed to the test cyclone are below 10 μm in diameter, and that particles above about 4 μm are completely removed. Particle size distributions were analyzed off-line down to 0.04 μm using a Coulter LS 230 laser sizer, after ultrasonic re-dispersion in ethanol.

Fig. 3 shows the grade efficiency curves obtained at different flow rates, where about 10–14% of the airflow was recirculated. It is clear that very high collection efficiencies were obtained, especially at the higher flow rates. The abnormal collection of very fine particles (below about 0.6 μm) had been observed before with RS_VHE and other HE cyclones, with and without recirculation, at both pilot and full scales for the capture of fine sulphanilic acid [6], as well as in larger diameter (≈1 m) cyclones and smaller diameter (≈0.20 m) multicyclones at biomass boilers [8]. This is attributed to capture of small particles by larger ones in the turbulent cyclone flow field, much as it happens in recirculating fluidized beds [14].

Fig. 4 shows a typical grade efficiency curve, together with the predictions from the complete collector–concentrator model. The agreement is very good down to about 1 μm, but the model over predicts collection between 0.6 and 1 μm, and clearly under predicts collection below 0.6 μm, most probably due to fine particle capture by larger ones, as referred above.

Grade efficiency curves were obtained sampling the total dust entering and exiting the recirculation system on GFA filters, and by weighing the filters on an analytical balance after proper drying. Thus, problems with anisokinetic sampling, which may occur with very small diameter sampling lines, were avoided.

While it may be argued that insufficient re-dispersion of fines from the Wright dust feeder, viz. agglomeration, is probably responsible for the general shape of the grade efficiency curves for submicron particles, experimental evidence at both laboratory, pilot and industrial scales shows that this is not so, as discussed in the next sections.

It should be stressed that no attempt was made to fit the turbulent dispersion coefficient in the model ($\mathcal{D}_r$) in order to get a better fit with the experimental values, and thus the value directly obtained from Eq. (1), computed for the median volume

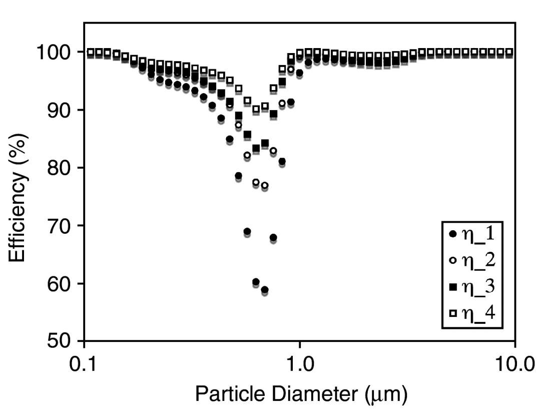

Fig. 3. Grade efficiency curves for $Ca(OH)_2$ (η_1 at 2.5e−4 m^3/s; η_2 at 3.2e−4 m^3/s; η_3 at 4.0e−4 m^3/s; η_4 at 4.8e−4 m^3/s).

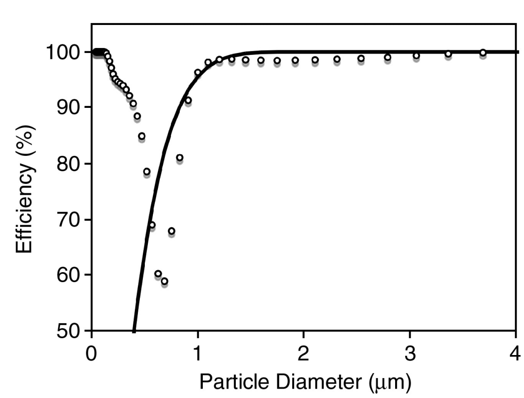

Fig. 4. Experimental and predicted grade efficiency for $Ca(OH)_2$ at 2.5e−04 m^3/s.

size, was employed. Fig. 5 shows that the global collections are under predicted, once more due to un-accounting in the model for the very high collections observed for particle diameters below about 0.6 μm, which in this particular case represent a sizeable mass fraction of the dust input to the cyclone.

4. Industrial scale experiments

4.1. Collection of sulphanilic acid and biomass boiler fly ash

A pilot scale test rig made up by one 0.45 m diameter RS_VHE cyclone (collector) and corresponding straight-through cyclone (concentrator) was installed at a manufacturer of sulphanilic acid. The test rig was run in parallel with a bag filter that collected the fines escaping from a process cyclone, which recycles the product to a fluidized bed dryer. The pilot system was designed to handle up to ≈1000 m^3/h of process gas and ≈500 m^3/h of recirculation gas, and particles at the test rig inlet had a size distribution with 17 μm median volume diameter and about 6% <1 μm. More details on the pilot rig can be found elsewhere [6,8]. The pilot recirculation system showed larger collection (≈99.4%) than the pulse jet bag filter (≈98.7%), and significantly larger than a competing high efficiency (HE) cyclone available on the marketplace (≈96.9%). Actually, the RS_VHE cyclone alone, without recirculation, clearly outperformed the HE cyclone and showed efficiencies up to 98.9%, viz., similar to the pulse jet bag filter. The recirculation system showed complete collection for particles above 8–10 μm [6].

Based on the excellent results of the pilot experiments, a full-scale facility of twelve 0.50 m cyclones and two concentrators was built for the recovery of sulphanilic acid from 14,000 m^3/h at 340 K, replacing the online pulse jet bag filter. A typical grade efficiency curve and the model predictions can be seen in Fig. 6. The recirculation fraction was kept at about 20%. Global collection reached 99.64% [6], with emissions in the range of 40–70 mg/Nm^3, mostly depending on inlet concentration. Once more, the model over predicts collection for a range of particle sizes (≈2–6 μm), and strongly under predicts below about 2 μm. Fig. 6 shows that the recirculation system is more efficient than the bag filter above about 3 μm, but also for extremely fine particles (<0.4 μm).

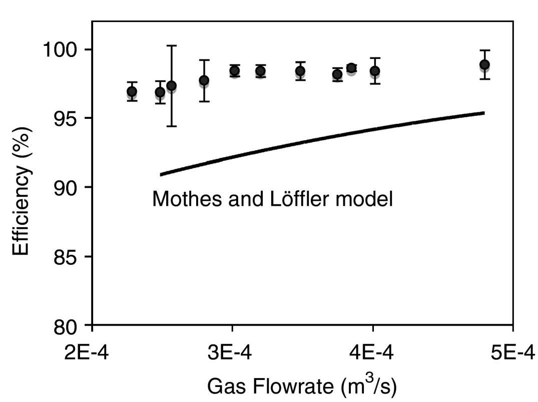

Fig. 5. Experimental (±95% c.i.) and theoretical efficiencies for lime at varying flow rates.

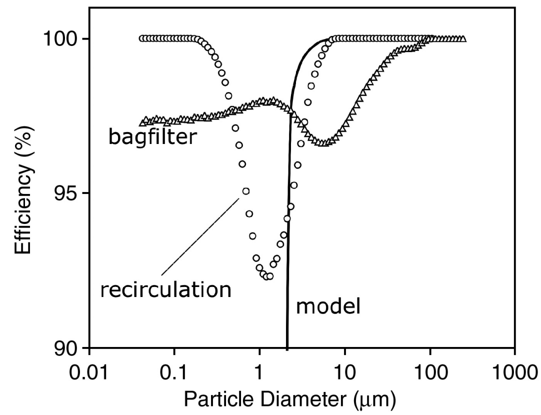

Fig. 6. Grade efficiencies for sulphanilic acid (concentration = 7.73 g/m^3, recirculation = 21.3%).

Since it was not possible to simultaneously perform sampling at both inlet and outlet of the systems, grade efficiency curves were obtained by isokinetic sampling at the system outlet (bag filter or recirculation system) and by simultaneously measuring the captured dust, using a process balance (precision ± 1%). Thus, errors due to sampling the inlet and outlet at different times, viz. at possible different process concentrations, were avoided. Particle size distributions were measured off-line for all samples using a Coulter LS230.

The dusts captured by the recirculation system and by the bag filter show all particle sizes present in the feed (see Ref. [6]), and since very fine particles are systematically absent from the emissions of the recirculation system but present on those of the bag filter, it must be concluded that fine particle capture occurs in the recirculation system by a mechanism that is absent (or not significant) in the bag filter. This is thought to be the capture by larger particles in the cyclone turbulent flow field, much like what occurs in recirculating fluidized beds [14]. For these high concentrations, it is known that fine particle capture is also strongly affected by the so-called mass loading effect, where a fraction of the incoming feed is removed unclassified in or before the inlet to the cyclone [15,16]. However, the mass loading effect shifts the entire grade efficiency curve upwards, so that there is a more or less uniform improvement in the collection of all particle sizes due to the effect of solid loading [15]. We show below that fine particle capture is also very high for much lower inlet concentrations for biomass boiler fly ash, both at pilot and industrial scales, and for airborne dust at pilot scale, thus apparently corroborating that turbulent particle dispersion could well be the dominant mechanism.

Biomass boiler emissions derived from cork and wood waste are very fine, typically with median volume diameters at 10–12 μm and with up to 10% submicrometer. Several RS_VHE recirculation facilities have been built for cork waste boilers with 0.50–0.70 m diameter cyclones, up to 50,000 m^3/h at 600 K. These systems have replaced single cyclones or multicyclone banks, which typically show efficiencies at the 40–60% level [8]. Global collection for the recirculation system for this application, with recirculated gas fractions of about 30%, is typically in the range of 93–96%, with emissions safely below 100 mg/Nm^3.

Grade efficiency curves obtained at two of the cork waste boilers and corresponding model predictions can be seen in Fig. 7. Once more, the model over predicts collection for a range of particle sizes, especially for the larger 0.70 m cyclones, and strongly under predicts below about 3–4 μm. Fig. 7 also shows that the multicyclone grade efficiencies are much lower than those from the optimized RS_VHE cyclones and corresponding recirculation system.

5. Emission particle size distributions

All grade efficiency curves reported above have been computed based on particle size distributions that were measured off-line, using a Coulter laser sizer with ultrasonic dispersion in an appropriate liquid (ethanol). It is important to know if these particle size distributions measured off-line are representative, and thus, if the computed grade efficiencies are meaningful.

To test this assumption, some experiments were conducted at a pilot scale test rig, similar to the one used for the sulphanilic acid experiments described above. The test powders were fine milled phosphorite (mean volume diameter = 12.5 μm) and wood waste ash (mean volume diameter = 11.2 μm), which were fed with a Topas 410H belt-driven venturi particle feeder. The particle feeder was calibrated by isokinetic sampling with GFA filters, and distributions sampled at the cyclone inlet were measured off-line with a Coulter sizer. Since these are identical to those of the bulk powders, it can be concluded that preferred particle deposition has not occurred upstream of the cyclone inlet. Simultaneous measurements at the clean side (stack) were performed using isokinetic gravimetric sampling on GFA filters followed by off-line sizing by a Coulter LS 230, and by isokinetic sampling using an online Grimm 1.108 laser monitor. This last device gives near instantaneous number distributions in 15 size channels, down to 0.27 μm, converted to mass distributions by appropriate calibration factors (the default factor, corresponding to a particle density of 2800 kg/m^3 was retained since this density is similar to that of phosphorite, 2750 kg/m^3 or wood boiler ash, 2790 kg/m^3).

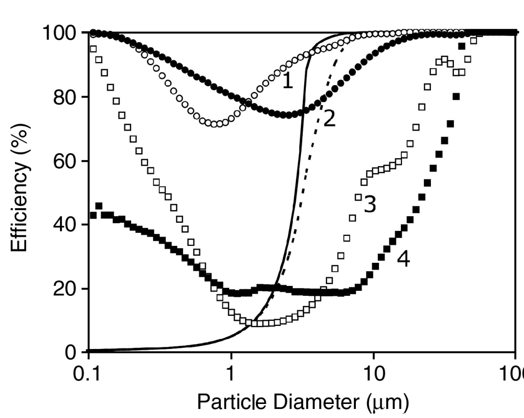

Fig. 7. Grade efficiencies for two cork waste boilers (concentrations < 1 g/m^3, recirculation = 30–33%; 1: 0.50 m cyclones and model (–); 2: 0.70 m cyclones and model (- -); 3 and 4: multicyclones.

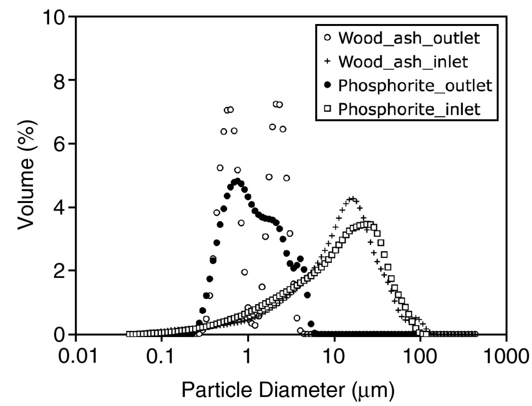

Fig. 8. Inlet and outlet distributions at pilot-scale recirculation system.

Fig. 8 shows typical inlet and outlet distributions obtained using phosphorite and wood waste ash, all measured by the off-line Coulter sizer. Both systems show a remarkable decrease in particle size after passing the recirculation system, and basically all particles above 6–8 μm have been removed from the gaseous stream. These results agree with those previously reported at full scale.

Fig. 9a and b show good agreement between the emissions' particle size distributions obtained by the off-line and online methods, both for phosphorite and wood–waste ash. However, the bimodality observed with the emissions from the wood–waste ash, and clearly seen in Fig. 8, is much more marked in the Coulter off-line measurements. These figures also show that the median size of the volume distribution exiting to the stack is extremely fine, with median volume diameter ≈ 1 μm.

Obviously, the good agreement on the emissions' particle size distributions by both the online and off-line methods is in no way proof that there are no agglomerates at the cyclone inlet, where concentrations are much higher. Unfortunately, the Grimm monitor could not be used in the full-scale cyclone plants due to the presence of acid gases and to temperature limitations (<323 K). Neither can it be used to measure inlet concentrations commonly encountered in cyclones, even if operated at ambient temperature, viz. in the pilot scale cyclone, both due to concentration (<100 mg/m^3) and particle size (<20 μm) constraints. Thus, grade efficiencies could not be fully determined for the pilot station for normally encountered concentrations based entirely on the online Grimm monitor information, but only on the Coulter off-line sizer.

Furthermore, there is some evidence that the Grimm monitor under predicts emissions with a relative error as large as 25%, since particles captured in the probe walls are not accounted for, contrary to the gravimetric isokinetic sampling, where the probe walls are flushed with an appropriate solvent. Thus, in order to use the Grimm monitor effectively for measuring emissions from the pilot station, prior calibration with isokinetic gravimetric sampling seems necessary.

6. Interpreting the shape of the grade efficiency curves

Several researchers have obtained grade efficiency curves in cyclones that show a minimum in collection, the so-called hook-

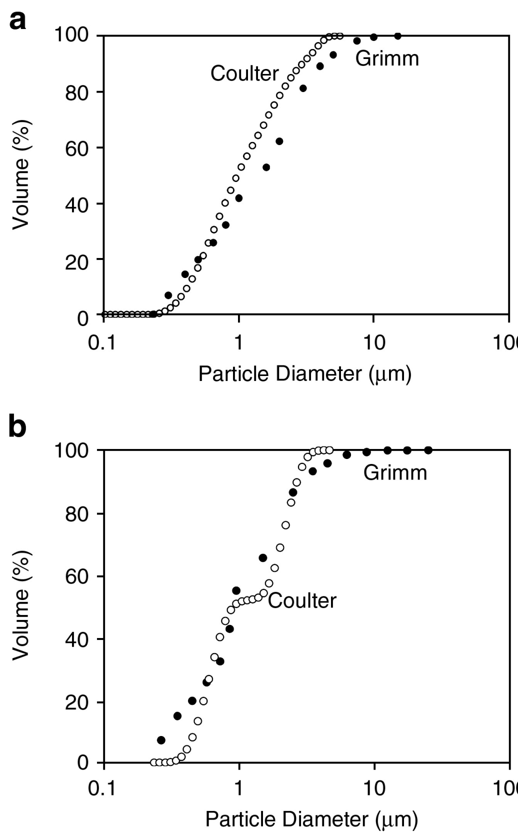

Fig. 9. a — outlet off-line and in-line distributions for phosphorite. b — outlet off-line and in-line distributions for wood–waste ash.

like or duck-tail curves [15–22]. These are variously attributed to a number of different factors, such as poor dispersion from powder feeders, collection of fine particles by larger ones in the cyclone turbulent flow field, turbulent particle dispersion bringing small particles to the cyclone wall, fine particle misplacement to the underflow due to blockage of their movement towards the inner vortex by larger particles, electrostatic forces and mass loading effects as discussed above.

We have shown before that these curves occur under a variety of different conditions: at laboratory scale using a Wright dust feeder [13], that compacts the dust prior to re-dispersion; at pilot scale using a Topas 410H belt-driven venturi particle feeder without dust compaction prior to re-dispersion; and at industrial scales where there are no particle feeders at all. The minima in the grade efficiency curves occur at moderately high (8 g/m^3) but also at low ($<$1 g/m^3) concentrations, and for a variety of different dusts, that probably have quite different interparticle forces.

It is unquestionable that if agglomeration occurs prior to the cyclone inlet, then smaller weight fractions of finer particles should be found in an online analysis as compared to off-line ones, due to a better dispersion in the liquid suspension in the latter [21]. While it cannot be ruled out that agglomeration prior to the cyclone inlet due to the particle feeder, when it exists, may be contributing to these minima, another more general hypothesis is here considered, viz. the role of turbulence, either by promoting collection of fine particles by larger ones [14,23,24] or by transporting fine particles to the cyclone wall [22].

Mao and Edwards [14] have studied the agglomeration in circulating fluidized bed absorbers, since a potential side benefit of these devices is the capture of fine particulate matter present in the flue gases by larger sorbent particles. These authors have built a model for particle agglomeration, considering different types, such as caused by brownian motion, by mean shear stress and by turbulence. For sorbent particles within 10–1000 μm (average radius 76 μm) and fine particles within 0.1–10 μm (average radius 2 μm), they found that turbulence is by far the main cause for fine particle losses to larger particles, and that this dominates over fine interparticle collision.

Hoffmann et al. [22] have generated grade efficiency curves by CFD and Lagrangian particle tracking, and studied the factors influencing the shape of these curves, comparing them with experimental data. This data includes hook-like (or duck-tail) grade efficiency curves, despite the fact that the test dust was premixed with a dispersant before being dispersed in compressed air through a sand blasting nozzle, at moderate solid loadings (5–20 g/m^3). These authors put forward the hypothesis that turbulent dispersion, which is stronger for smaller particles, may bring these to the cyclone wall, where they are collected. Both models used predict a minimum in the grade efficiency curves, despite the fact that neither the shape of the curve nor the position of this minimum is well predicted. These authors then conclude that the shape of the tailing in the experimental curves is probably due to small particles being collected as agglomerates, but the uncertainty remains if these are formed in the cyclone or never being broken up in the feed.

Chi and Sommerfeld [23] have modeled turbulent particle transport and particle collision and agglomeration, using a stochastic Lagrangian agglomeration model. For particles in the range 1–20 μm, these authors state that after a short time (5 s), most of the particles below 5 μm have been collected by the larger particles, concluding that the probability of agglomeration between large particles is zero, but it is very high between small and large particles. Using as model parameters turbulence intensities typical of cyclone collectors, and initial particles within the range 1–62 μm, they concluded that after about 0.02 s all particles below 10 μm were collected by the larger particles, and that the smaller the particle density the larger the rate of agglomeration.

Sommerfeld and Chi [24] have applied the stochastic Lagrangian agglomeration model [23] to a 190 mm standard cyclone, predicting that small particles are collected by larger particles, and therefore separated.

All experimental grade efficiency curves shown so far in this work were obtained using an off-line laser sizer, since, as explained above, the in-line laser monitor could not be used with typical inlet concentrations, neither at the operating conditions of industrial processes. To experimentally validate that small particles are indeed collected in the recirculating cyclones with much higher efficiency than expected, and that this is neither an artifact of the off-line measuring technique nor of poor dispersion prior to the cyclone inlet, two simple experiments were conducted with airborne particles in the pilot scale test rig described in Section 5. The idea is that by using airborne particles, no feeder is employed, and since inlet concentrations are very low, typically below 150 μg/m^3, then mass loading effects are certainly absent. Under these low loads, the in-line laser sizer can be used for both inlet and outlet concentration measurements, bypassing the need to use liquid dispersion. The only drawback of this method is that it was not possible to simultaneously measure the inlet and the outlet, although all care was taken to accept measurements that showed a near constant size distribution and concentration at both sampling ports over an appreciable length of time (about 1 h). This is needed since there is no actual control over airborne particle concentration and/or its size distribution.

Fig. 10a shows the inlet distributions for the two experiments, Fig. 10b shows the corresponding outlet distributions and Fig. 11 the corresponding grade efficiency curves, together with model predictions.

Fig. 10a shows that the mass size distributions of these two experiments are similar, with median mass diameters at 1.76–2.27 μm, and about 37% submicrometer, at inlet concentrations from 56–136 μg/m^3. Since the density of these airborne particles is not known, it was assumed that they are road and soil eroded particles, and a density of 2200 kg/m^3 was assigned to them. This is needed by the laser monitor for conversion to a mass-basis measurement, but also by the model. Thus, the size distributions should be considered only as approximate, as different particle sizes can have different chemical composition and thus different density.

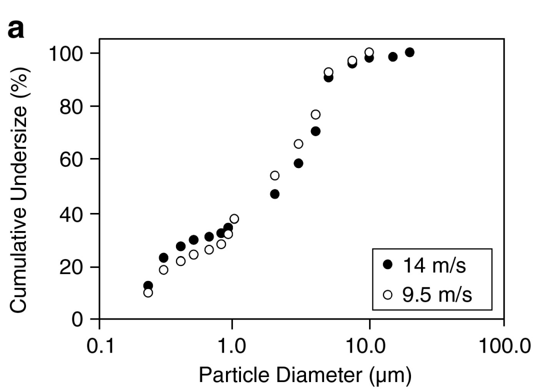

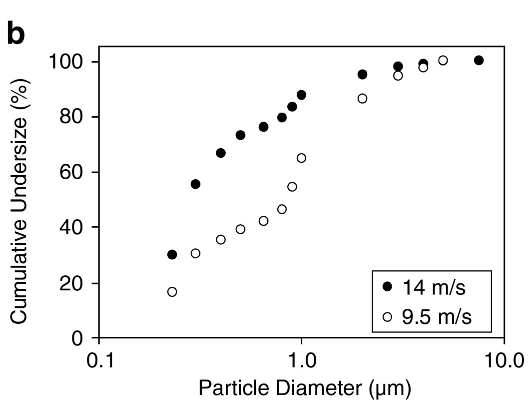

Fig. 10. a — inlet in-line distributions for airborne dust. b — outlet in-line distributions for airborne dust.

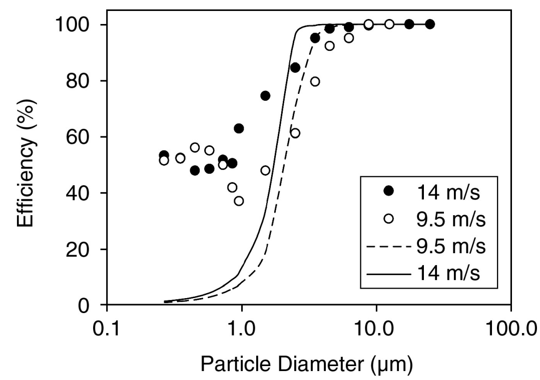

Fig. 11. Grade efficiency curves for airborne dust model at 9.5 m/s (–); model at 14 m/s (–).

Fig. 10b shows that the outlet distributions are very different, with a much finer distribution at higher velocity (0.29 μm median mass diameter against 0.85 μm), corresponding to a much higher global collection efficiency (80.4% against 70.7%). In these experiments the recirculation fraction (rr) was kept at about 34%, and a higher collection should be expected at higher velocities [6].

Fig. 11 shows that, below 2.5 μm, the experimental grade efficiencies are much larger than predicted by the model, and that the deviations are stronger for the higher gas velocity. The experimental curves show a minimum at submicrometer sizes, deviating to a smaller particle size at higher gas velocity.

From the possible causes of the high collection of fine particles discussed above, only two appear to be possible under these experimental conditions: collection by larger ones in the cyclone turbulent flow field, or turbulent particle dispersion bringing small particles to the cyclone wall. It is also evident that much research still needs to be done before a definite conclusion can be made.

7. Conclusions

This paper presents results obtained at laboratory, pilot and industrial scales of the behavior of numerically optimized gas cyclones, when coupled to a partial recirculation system within a collector (reverse-flow cyclone) upstream from the concentrator (straight-through cyclone). The following conclusions can be taken:

i) Grade efficiency curves for the recirculation system were generated by extending the Mothes and Löffler model [11] to the concentrator, and the agreement with experimental data is reasonable when the particles' turbulent dispersion coefficient is estimated through an empirical relation [3], except for fine particles, which are collected to a much higher extent than predicted.
ii) The generally observed high collection of fine particles is attributed to their capture by turbulent dispersion by larger particles within the cyclone flow field, similar to what occurs in recirculating fluidized beds [14]. However, agglomerates at the cyclone inlet cannot be ruled out, and further experiments should be conducted to determine to

what extent these might contribute for the observed minima in the grade efficiency curves.

iii) The proposed systems are much more efficient than multicyclones operating in waste biomass boilers, despite the fact that multicyclones have much smaller diameters.

iv) The results so far obtained open the applicability of these devices to collection efficiencies typical of more costly de-dusters, such as online pulse jet bag filters and electrostatic precipitators. However, the results also suggest that this will only occur for fine particles if the particles to be removed have a relatively wide size distribution, otherwise the fine particles will not have larger particles to act as collection targets in the turbulent flow field. For high inlet dust concentrations such as occurring in the sulphanilic acid experiments, the collection mechanism of fine particles may be dominated by the mass loading effect [15].

v) Particle size distributions measured at the clean (stack) side of the recirculation system show a good agreement between online and off-line measurements, and an excellent agreement between median volume diameters, which are in the range of 1 to 1.5 μm.

vi) Emissions computed with an online monitor may be in error, since particles that are lost to the probe walls are not accounted for.

vii) Experiments at pilot scale with airborne dust at very low concentrations (≈100 μg/m^3) show that fine particle collection, below about 2.5 μm, is also much higher than theoretically expected, with a minimum in the submicron range. This seems to indicate that turbulent dispersion plays an important role in determining fine particle collection for cyclone recirculating systems, either by fine particle capture by larger ones [14,23,24] or by bringing fine particles near the cyclone wall [22].

List of symbols

d_p	Particle diameter, m
h	Height of cylinder portion of reverse-flow cyclone (or length of region 4 in concentrator), m
l	Natural cyclone length, m
r_a	Cyclone or concentrator radius, m
r_a^*	Equivalent radius for cylindrical model of reverse-flow cyclone, m
r_i	Vortex radius (or radius in region 4), m
rr	Recirculation fraction
s	Vortex height (or axial length height in concentrator), m
ss	Axial inlet length in concentrator, m
v_d	Mean barrel velocity, m.s^{-1}
v_r	Radial gas velocity, m.s^{-1}
v_φ	Tangential velocity, m.s^{-1}
$v_{\varphi a}$	tangential velocity near the wall, m.s^{-1}
C_i	Particle concentration in region i, kg.m^{-3}
$\mathcal{D}_r$	Particle turbulent dispersion coefficient, m^{2}s^{-1}
H	Total cyclone and concentrator height, m
K	Angular momentum parameter
$\mathrm{Pe_p}$	Particle radial Peclet
Re_p	Particle radial Reynolds
$\dot{V}_i$	Volumetric flow in region *i,* m^3 s^{-1}
ρ	Gas density, kg.m^{-3}
ρ_p	Particle density, kg.m^{-3}
μ	Gas viscosity. kg.m^{-1}s^{-1}
ξ	Apparent friction factor
ω	Particle (radial) terminal velocity, m.s^{-1}

Acknowledgements

The authors thank FCT (Portuguese Foundation for Science and Technology) for financial support through contracts POCTI /EQU/37992/2001 (FEDER contribution) and BD 8191/2002.

References

[1] F.A. Zenz, Cyclone design tips, Chem. Eng. (New York) 108 (1) (January 2001) 60.

[2] R.L. Salcedo, J.A.G. Campos, Optimization for pollution reduction: a numerical approach to cyclone design, 2nd Conference on Process Integration, Modeling and Optimization for Energy Saving and Pollution Reduction, Veazprém, Hungary, vol. 571, ISBN: 963 8192 87 9, 1999.

[3] R.L. Salcedo, M.A. Coelho, Turbulent dispersion coefficients in cyclone flow — an empirical approach, Can. J. Chem. Eng. 77 (August 1999) 609.

[4] R.L. Salcedo, M.G. Cândido, Global optimization of reverse-flow gas-cyclones: application to small-scale cyclone design, Sep. Sci. Technol. 36 (12) (2001) 2707.

[5] R.L. Salcedo. High Efficiency Cyclones, European Patent 0972572, European Patent Bulletin, 2000, March.

[6] R.L. Salcedo, M.J. Pinho, Pilot and industrial-scale experimental investigation of numerically optimized cyclones, Ind. Eng. Chem. Res. 42 (1) (2002) 145.

[7] R. L. Salcedo. Recirculation cyclones for dedusting and dry gas cleaning, US Patent 2002178793, *United States Patent Application Publication*, 2002, December.

[8] R.L. Salcedo, V.G. Chibante, I. Sôro, Laboratory, pilot and industrial-scale validation of numerically optimized reverse-flow gas cyclones, Trans. Filtr. Soc. 4 (3) (2004) 220.

[9] R. Clift, M. Ghadiri, A.C. Hoffman, A critique of two models for cyclone performance, AIChE J. 37 (1991) 285.

[10] R. Salcedo, A.M. Fonseca, Grade-efficiencies from sampling cyclones, in: N.P. Cheremisinoff (Ed.), Mixed-Flow Hydrodynamics — Advances in Engineering Fluid Mechanics Series, vol. 23, Gulf Publishing Co, ISBN: 8894152561, 1996, pp. 539–561.

[11] H. Mothes, F. Löffler, Prediction of particle removal in cyclone separators, Int. Chem. Eng. 28 (1988) 231.

[12] R. Wysk, L.A. Smolensky, Novel particulate control device for industrial cleaning, Filtr. Sep. 29 (Jan–Feb 1993).

[13] B.M. Wright, A new dust-feed mechanism, J. Sci. Instrum. 27 (1953) 12.

[14] D. Mao, J.R. Edwards, A.V. Kuznetsov, R. Srivastava, A model for fine particle agglomeration in circulating fluidized bed absorbers, Heat Mass Transf. 38 (2002) 379.

[15] A.C. Hoffmann, L.E. Stein, Gas Cyclones and Swirl Tubes — Principles, Design and Application, vol. 6, Springer-Verlag, Berlin Heidelberg, New York, 2002.

[16] A.C. Hoffmann, A. van Santen, R.W.K. Allen, R. Clift, Effects of geometry and solid loading on the performance of gas cyclones, Powder Technol. 70 (1992) 83.

[17] R.L. Salcedo, Collection efficiencies and particle size distributions from sampling cyclones — comparison of recent theories with experimental data, Can. J. Chem. Eng. 71 (February 1993) 20.

[18] A.C. Hoffmann, M. de Groot, A. Hospers, The effect of the dust collection system on the flowpattern and separation efficiency of a gas cyclone, Can. J. Chem. Eng. 74 (August 1996) 464.
[19] C.J. Stairmand, The design and performance of cyclone separators, Trans. Inst. Chem. Eng. 29 (1951) 356.
[20] K.T. Hsieh, R.K. Rajamani, Mathematical model of the hydrocyclone based on physics of fluid flow, AIChE J. 37 (1991) 735.
[21] M.B. Ray, A.C. Hoffmann, R.S. Postma, Performance of different analytical methods in evaluating grade efficiency of centrifugal separators, J. Aerosol Sci. 31 (5) (2000) 563.
[22] A.C. Hoffmann, A. Berrino, M.B. Ray, On the shape of grade efficiency curves computed for centrifugal dedusters by CFD with Lagrangian particle tracking, AIChE Symp. Ser. 321 (95) (1999) 13.
[23] C.A. Ho, M. Sommerfeld, Modelling of micro-particle agglomeration in turbulent flows, Chem. Eng. Sci. 57 (2002) 3073.
[24] M. Sommerfeld, C.A. Ho, Numerical calculation of particle transport in turbulent wall bounded flows, Powder Technol. 131 (2003) 1.